

$T$	temperature, K
$t$	temperature, °C
$v$	molar volume, cm <sup>3</sup> /mol
$x_i$	liquid-phase mole fraction of component $i$
$y_i$	vapor-phase mole fraction of component $i$
$g_{ij}, u_{ij}, \lambda_{ij}$	interaction parameter between components $i$ and $j$
$\alpha$	nonrandomness parameter
$\gamma_i$	activity coefficient of component $i$

Registry No. Tetrahydrofuran, 109-99-9; ethanol, 64-17-5.

#### Literature Cited

- (1) Horsley, L. H. "Azeotropic Data III"; American Chemical Society: Washington, DC, 1973; *Adv. Chem. Ser.* No. 116.
- (2) Yoshikawa, Y.; Takagi, A.; Kato, M. *J. Chem. Eng. Data* 1980, 25, 344.

- (3) Bernshtein, L. A.; Generalova, T. V.; Zelvenskii, Y. D.; Shalygin, V. A. *J. Appl. Chem. USSR (Engl. Transl.)* 1980, 53, 1577 (*Zh. Prikl. Khim.* 1980, 53, 2115).
- (4) Hunsmann, W. *Chem.-Ing.-Tech.* 1967, 39, 1142.
- (5) Brunner, E.; Scholz, A. G. R. *Chem.-Ing.-Tech.* 1980, 52, 164.
- (6) Wilson, G. M. *J. Am. Chem. Soc.* 1964, 86, 127.
- (7) Renon, H.; Prausnitz, J. M. *AIChE J.* 1968, 13, 135.
- (8) Abrams, D. S.; Prausnitz, J. M. *AIChE J.* 1975, 21, 116.
- (9) Gmehling, J.; Onken, U. "Vapor-Liquid Equilibrium Data Collection"; DECHEMA: Frankfurt, 1977; DECHEMA Chemistry Data Series, Vol. 1, Part 1.
- (10) Anderson, T. F.; Abrams, D. S.; Grens, E. A. *AIChE J.* 1978, 24, 20.
- (11) Boublik, T.; Fried, V.; Hala, E. "The Vapor Pressures of Pure Substances"; Elsevier: Amsterdam, 1973.
- (12) Scott, D. W. *J. Chem. Thermodyn.* 1970, 2, 833.
- (13) "Selected Values of Properties of Chemical Compounds"; Thermodynamics Research Center Data Project, Texas A & M University: College Station, TX.

Received for review December 15, 1982. Revised manuscript received May 13, 1983. Accepted July 15, 1983.

## Measurements of the Vapor-Liquid Coexistence Curve for the Binary R12 + R22 System in the Critical Region

Yukihiko Higashi, Shiro Okazaki, Yoshinori Takahashi, Masahiko Uematsu,\* and Koichi Watanabe

Department of Mechanical Engineering, Keio University, Yokohama 223, Japan

Measurements of the vapor-liquid coexistence curve in the critical region for the binary dichlorodifluoromethane (CCl<sub>2</sub>F<sub>2</sub>, R12) + chlorodifluoromethane (CHClF<sub>2</sub>, R22) system were made by visual observation of the disappearance of the meniscus at the vapor-liquid interface within an optical cell. Fifty-one saturated-vapor densities and thirty-seven saturated-liquid densities for seven different compositions of 0, 10, 20, 30, 50, 75, and 100 wt % R22 between 355 and 385 K ( $T_r > 0.96$ ) were obtained in the range of densities 260-892 kg/m<sup>3</sup> ( $0.5 < \rho_r < 1.5$ ). The experimental error of temperature, density, and mass fraction was estimated within  $\pm 10$  mK,  $\pm 0.5\%$  and  $\pm 0.05\%$ , respectively. The composition dependence of the critical parameters is analyzed and discussed on the basis of these measurements.

Although nonazeotropic binary mixtures have recently been considered to be prospective working fluids for refrigeration and heat pump cycles, only limited information about the thermodynamic properties of these substances is available. A binary dichlorodifluoromethane (R12) + chlorodifluoromethane (R22) system is assigned to the refrigerant number of 501 for a mixture of 75 wt % R22. However, Kriebel (1) measured the phase equilibria for the R12 + R22 system over the whole range of compositions between 213 and 343 K. He found that the azeotropic composition for this system shifts from 84.5 wt % R22 at 231.65 K to 100 wt % R22 at 258.65 K, above which this system forms no more azeotrope.

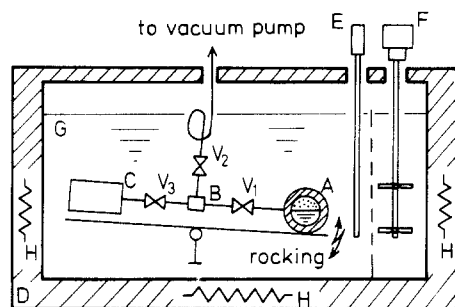
We have carried out systematically a thermodynamic investigation on this R12 + R22 system. The  $PVT_x$  measurements were reported (2, 3) and the composition dependence of the thermodynamic state surface (4) as well as an analysis on the application to the refrigeration cycle (5) was also discussed. This paper reports measurements of the vapor-liquid coexistence curve for seven different compositions, i.e., 0, 10, 20, 30, 50, 75, and 100 wt % R22, by visual observation of the disappearance of the meniscus at the vapor-liquid interface. The composition dependence of the critical parameters including

those for both pure components is also reported.

#### Experimental Section

The vapor-liquid coexistence curve for a certain composition of the binary R12 + R22 system was measured by observing the behavior of the meniscus at the vapor-liquid interface in an optical cell. The experimental apparatus used and the principle of the measurements were described in detail in a previous publication (6). With the aim of measuring saturation temperatures for a series of densities along the coexistence curve of a fixed composition successively, we introduced the expansion technique into the meniscus observation. The optical cell was connected with an expansion vessel for repeating expansion procedures from the optical cell to the expansion vessel after the measurement of a saturation temperature. Additionally, another vessel called a supplying vessel was connected with the optical cell and the expansion vessel as shown schematically in Figure 1, which allowed the sample fluid in the supplying vessel to be supplied to the optical cell after completion of a single series of expansion procedures. Careful attention was paid to the expansion procedure in order not to change the sample composition. We performed the expansion procedures at a state where the sample fluid was kept under the homogeneous phase at a constant temperature. In the meantime these three vessels were rocked to homogenize the sample density and composition.

The optical cell was a cylindrical vessel made of 304 stainless steel (50 mm long and 19 mm in inner diameter, 15 cm<sup>3</sup> in inner volume) with two synthetic sapphire windows (15 mm in thickness) using Teflon O rings and Teflon packings for the high-pressure seal. We calibrated the inner volume of the cell by filling the water with known density values under room-temperature conditions with an uncertainty of 0.03%, whenever we disassembled the cell and reassembled it. In this study, the cell was disassembled 4 times due to experimental trouble and reassembled by using new packings. The inner volume of the cell was calibrated each time and the results were  $14.973 \pm 0.005$ ,  $15.176 \pm 0.005$ ,  $15.153 \pm 0.004$ , and  $15.067 \pm 0.005$



- A : Optical cell  
 B : Expansion vessel  
 C : Supplying vessel  
 D : Thermostated bath  
 E : Platinum resistance thermometer  
 F : Stirrer  
 G : Heat transfer medium  
 H : Electric heater  
 $V_1, V_2, V_3$  : Valves

Figure 1. Schematic setup of the apparatus.

$\text{cm}^3$ , respectively. The expansion vessel and the supplying vessel were also cylindrical and made of 304 stainless steel. Their inner volumes were  $7.355 \pm 0.005$  and  $77.052 \pm 0.005$   $\text{cm}^3$ , respectively.

After the sample fluid whose mass was  $m$  and composition  $x$  was prepared in the supplying vessel, the three vessels were assembled and immersed into a thermostated bath where liquid paraffin oil was used as a heat-transfer medium. When the optical cell and the expansion vessel were evacuated under vacuum to around 0.5 mPa, the sample fluid in the supplying vessel was then expanded into the optical cell and the expansion vessel. By this procedure, the sample fluid of density  $\rho(1,0)$  occupied the optical cell after the three valves  $V_1$ ,  $V_2$ , and  $V_3$  were closed. After completion of the measurement for the density  $\rho(1,0)$ , the valve  $V_2$  connecting to the vacuum pump was opened so as to discharge the sample fluid from the expansion vessel for the evacuation while the other two valves  $V_1$  and  $V_3$  were closed. Then the sample fluid within the optical cell was expanded only into the expansion vessel and now the sample fluid with density  $\rho(1,1)$  occupied the optical cell. Similarly, for the density  $\rho(1,0)$ , the saturation temperature corresponding to  $\rho(1,1)$  was determined.

By combination of these two expansion procedures, i.e., expansion of the sample fluid to the optical cell and the expansion vessel from the supplying vessel and that to the expansion vessel from the optical cell, almost infinite measurements may be performed by a single filling of the sample fluid into the supplying vessel as far as the theory is concerned. After completing the expansion from the supplying vessel  $N_p$  times and that from the optical cell  $N_s$  times, one can express density  $\rho(N_p, N_s)$  of the sample fluid by the equation

$$\rho(N_p, N_s) = mV_A^{N_p}V_C^{(N_p-1)} / \{(V_A + V_B + V_C)^{N_p}(V_A + V_B)^{N_s}\} \quad (1)$$

where  $N_p$  is an arbitrary integer starting from unity and  $N_s$  from zero.  $V_A$ ,  $V_B$ , and  $V_C$  denote the inner volume of the optical cell, the expansion vessel, and the supplying vessel, respectively. These volumes should be corrected with respect to the thermal expansion and the pressure deformation. The temperature effect was correlated by using the available information about the temperature dependence of the linear thermal expansion coefficient for 304 stainless steel, whereas the pressure effect even under the inner pressure of 5 MPa is found to be much less than 1/27 of the effect due to the thermal expansion according to theoretical stress analysis with respect to the cylindrical vessel. In the present study, the experimental pressure never exceeded 5 MPa, and hence we have concluded that the pressure effect is negligible in the present

analysis, while the thermal expansion was corrected exclusively. Here the thermal expansion of the optical cell was calculated on the assumption that the optical cell was made of only 304 stainless steel. The extent of correction concerning the inner volume of the optical cell thus calculated was only about 0.5% of its volume under the most severe conditions.

Although, with this method, we can obtain a considerable quantity of data by a single filling of the sample fluid, it is unavoidable that the experimental error with respect to the measured density becomes larger proportionally with the total number of expansion procedures. Hence, in the present study, we restricted the expansion procedures until  $N_p \leq 3$  as well as  $N_s \leq 2$  corresponding to each single expansion from the supplying vessel so as to maintain the error of the measured density within 0.5%.

The temperature measurements were conducted with a 25- $\Omega$  platinum resistance thermometer (Chino: Model R800-1) calibrated with a precision of 5 mK on IPTS-68 at the National Research Laboratory of Metrology, Ibaraki, Japan, with the aid of a Mueller-type bridge (Shimadzu: type BD-100). The thermometer was mounted in the vicinity of the optical cell at the same level in the thermostated bath. Since the sample temperature was not measured directly, full attention was paid to confirm thermodynamic equilibrium between the sample fluid and the thermostated bath fluid during the experiments. The bath temperature was kept constant within the fluctuation of  $\pm 3$  mK. The possible uncertainty in the temperature measurements is estimated within  $\pm 10$  mK including the precision of the thermometer used, the fluctuation of temperature controlled, and an individual difference with respect to the temperature determination of the disappearing meniscus, i.e., 2–3 mK.

For the preparation of the sample fluid with a prescribed density and composition, additional cylindrical vessels similar to the supplying vessel were used to fill each of them with respective components. These cylindrical vessels were also made of 304 stainless steel. The suitable mass of respective components filled in each vessel was weighed on a precision chemical balance (Chyo: Model C2-3000) with an uncertainty of 2 mg. Then each component was transferred successively into the supplying vessel which was evacuated in advance up to around 0.5 mPa and well cooled by liquefied nitrogen. The purities of both components used were 99.99 wt % pure R12 ( $\text{CCl}_2\text{F}_2$ ) and 99.99 wt % pure R22 ( $\text{CHClF}_2$ ). We estimated that the uncertainty of the mass fraction of the sample mixture thus prepared was not greater than  $\pm 0.05\%$ .

## Results

The experimental temperature–density data along the coexistence curve for seven different compositions of 0, 10, 20, 30, 50, 75, and 100 wt % R22 are given in Table I and illustrated in Figure 2. These 88 measurements cover the temperature range from 355 to 385 K ( $T_r > 0.96$ ) and the density range from 260 to 892  $\text{kg/m}^3$  ( $0.5 < \rho_r < 1.5$ ). The values with an asterisk in Table I were obtained when the meniscus disappeared and the critical opalescence was observed simultaneously. The critical opalescence observed was distinguished due to the density measured. For the measurements at densities that were larger than the critical density  $\rho_c$ , i.e.,  $\rho > \rho_c$ , the critical opalescence at the vapor phase was observed more intensively than that at the liquid phase, while the meniscus ascended and disappeared prior to reaching the top of the optical cell with increasing temperature. For  $\rho < \rho_c$ , however, the critical opalescence at the liquid phase was observed more intensively, while the meniscus descended and disappeared prior to reaching the bottom of the optical cell with increasing temperature. For the densities in the very vicinity of the critical point, the critical opalescence at the vapor phase was observed as intensively as that at the liquid phase, while the meniscus

Table I. Measured Data along the Coexistence Curve for the R12 + R22 System<sup>a</sup>

T, K	$\rho$ , kg/m <sup>3</sup>	T, K	$\rho$ , kg/m <sup>3</sup>
R12			
374.359	260.4	384.943	475.0
375.205	270.9	384.953	496.0*
377.390	290.6	385.008	520.2*
378.303	301.1	385.012	570.5*
379.868	319.3	384.973	599.6*
382.731	375.4	384.895	640.9*
383.203	388.2	383.931	706.9
383.504	403.0	383.071	746.7
384.216	431.5	381.884	774.2
384.656	448.8	379.188	828.4
10.00 wt % R22			
378.037	352.4	381.537	597.5*
379.384	378.0	381.609	651.6
380.709	400.7	380.748	690.8
381.625	436.9	377.410	783.7
381.874	463.3	374.155	840.7
381.576	525.5*	370.156	891.5
381.698	563.5*		
20.03 wt % R22			
373.173	300.0	378.751	576.8*
376.750	358.1	378.661	617.3*
378.716	447.2*	377.900	667.0
378.813	478.6*	373.277	796.4
378.797	533.9*	368.968	860.6
30.00 wt % R22			
369.897	295.2	375.908	567.6*
374.362	380.6	375.349	656.2*
375.643	440.1	367.257	846.7
376.012	508.8*		
50.00 wt % R22			
366.066	292.1	372.317	561.6*
370.469	376.6	371.966	649.3*
372.093	435.4	367.637	775.3
372.317	503.4*	363.459	837.8
75.00 wt % R22			
364.052	282.4	369.873	543.1*
368.164	364.2	369.350	627.9
369.415	421.1	362.400	810.1
R22			
361.382	266.1	369.318	511.5*
364.021	297.4	369.320	523.3*
364.640	307.6	369.296	543.0*
365.877	325.9	369.283	570.5*
366.701	343.1	369.254	591.4*
367.502	364.9	368.838	625.9
368.050	384.3	368.326	655.4
368.315	396.6	367.856	675.6
368.874	420.6	364.237	763.0
369.138	441.4	361.379	808.4
369.218	458.6*	358.190	847.4
369.289	484.8*	355.676	872.1

<sup>a</sup> Values with an asterisk were measured by observing the critical opalescence.

ascended or descended very slightly and disappeared near the middle of the optical cell with increasing temperature. In the case of the critical density, the meniscus level is kept unchanged at the middle of the optical cell with increasing temperature. And then the vapor-liquid interface becomes indistinguishable and finally disappears at the critical temperature, where the critical opalescence is observed most intensively. No significant difference between the pure substances and mixtures with respect to the meniscus disappearance as well as the intensity of critical opalescence was observed.

On the basis of the present measurements along the vapor-liquid coexistence curve, we determined the critical temperature  $T_c$  and density  $\rho_c$  for the respective compositions by analyzing these data taking into consideration the disappearing

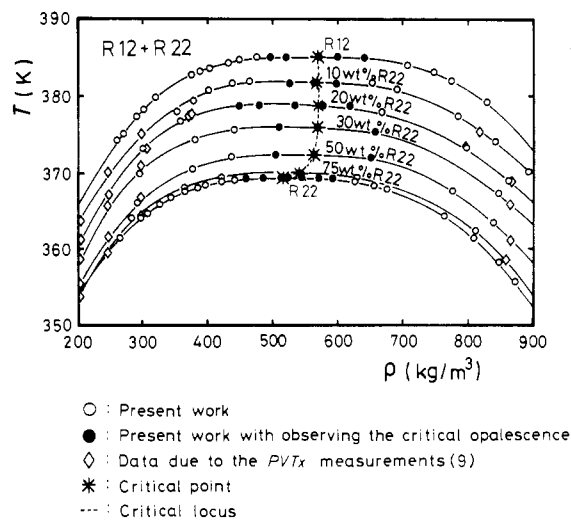


Figure 2. Experimental results for the R12 + R22 system.

Table II. Critical Parameters for the R12 + R22 System

composition of R22				
$w_1$ , wt %	$x_1$ , mol %	$T_c$ , K	$\rho_c$ , kg/m <sup>3</sup>	$P_c$ , MPa
0	0	385.01 ± 0.01	568 ± 3	4.129 ± 0.008
10.00	13.45	381.68 ± 0.05	567 ± 5	4.28 ± 0.03
20.03	25.94	378.76 ± 0.03	569 ± 10	4.43 ± 0.03
30.00	37.47	375.91 ± 0.01	568 ± 3	4.54 ± 0.03
50.00	58.30	372.32 ± 0.01	562 ± 3	4.74 ± 0.03
75.00	80.75	369.87 ± 0.02	540 ± 5	4.88 ± 0.03
100	100	369.32 ± 0.01	515 ± 3	4.990 ± 0.005

meniscus level and the intensity of the critical opalescence. The critical pressure  $P_c$  was determined by using either the published vapor pressure data or correlations with the present value of  $T_c$ . As for the pure components, we calculated each value of  $P_c$  from the correlations given in the tables of thermophysical properties for R12 (7) and in those for R22 (8) published by the Japanese Association of Refrigeration. As for the mixtures, we determined each value of  $P_c$  for the respective compositions graphically with the aid of the  $PVTx$  measurements by Takaishi (9). The critical parameters thus obtained are given in Table II. The mass fraction of each composition for the mixtures measured was converted into the mole fraction by using the molar mass of 120.914 g/mol for R12 and that of 86.469 g/mol for R22. We estimated the uncertainty of the critical parameters one by one for each composition as listed in Table II, because the uncertainty is composed of not only the experimental error but also that due to the present process of determining the critical parameters. The latter depends on the density dependence of the coexistence curve, the behavior of the disappearing meniscus, and the number of data used. The uncertainty of  $T_c$  for the 10 wt % R22 mixture being the largest is mainly due to the density dependence of the coexistence curve. The uncertainty of  $\rho_c$  for the 20 wt % R22 mixture being the largest is mainly due to the behavior of the meniscus disappeared. The uncertainty of  $P_c$  for mixtures being larger than that for both pure components is due to the shortage of the data used.

The critical points for the respective compositions and the critical locus are illustrated on a temperature-density plane in Figure 2 and on a pressure-temperature plane in Figure 3. The thermodynamic state surface of the vapor-liquid coexistence state for the R12 + R22 system in the critical region is projected onto a molar volume-composition plane in Figure 4. The isotherms and isobars in this figure were determined in the present results with the aid of the  $PVTx$  measurements by Takaishi (9).

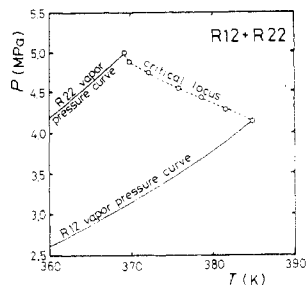


Figure 3. Critical locus for the R12 + R22 system.

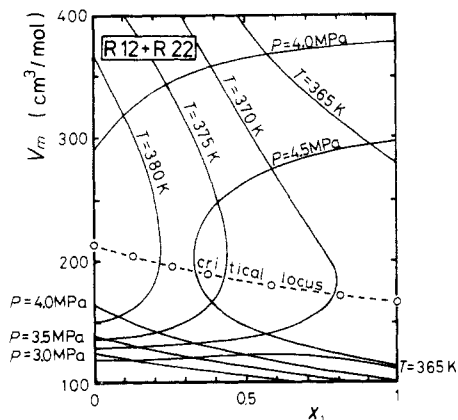


Figure 4. Isotherms, isobars, and critical locus for the R12 + R22 system.

### Discussion

Takaishi (9) analyzed his own  $PVTx$  measurements and determined graphically the temperature and pressure values for his isochores at their intersecting points with the coexistence curve, which are also shown in Figure 2. These data and the coexistence curves generated are quite coincident with the present measurements, although these two experiments were carried out independently. In Figure 2 the maxcondentherm points of the R12 + R22 system were observed at densities smaller than  $\rho_c$ . The maximum temperature of the coexistence curve for the 10 wt % R22 mixture is higher than its  $T_c$  by about 0.2 K, which is the largest temperature difference between the maxcondentherm points and the critical points for this system. The temperature differences for 20 wt % R22 and 30 wt % R22 mixtures are about 0.1 K, whereas no significant differences for the mixtures of other compositions are observed.

The shape of the coexistence curves on the  $T-\rho$  plane for the mixtures of this system shown in Figure 2 is similar to those for both pure components in the density region of 200–900  $\text{kg}/\text{m}^3$ . Particularly the coexistence curve of the 75 wt % R22 mixture is close enough to that of pure R22 and  $T_c$  of this mixture is higher than  $T_c$  of R22 by 0.55 K. The critical locus for this system on the  $P-T$  plane shown in Figure 3 becomes concave and the pressure of the locus decreases with increasing temperature. The locus does not intersect the vapor pressure curve of R22 and it is hard to expect that  $T_c$  of any mixtures between 75 and 100 wt % R22 might be lower than  $T_c$  of R22. In our previous work on the  $PVTx$  measurements for this system (2), we found that the temperature difference between the dew and bubble points at a given pressure for a mixture of 75 wt % or more R22 is very small, but both temperatures are not lower than the saturation temperature of pure R22 as far as the region of the measurements being over 2.5 MPa is concerned. Hence, the present R12 + R22 system does not form an azeotrope in the region of pressures above 2.5 MPa. It is expected that the coexistence curves on the

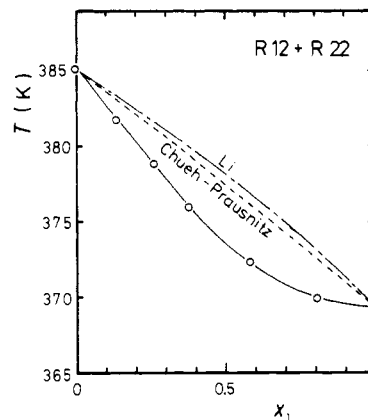


Figure 5. Composition dependence of the critical temperature for the R12 + R22 system.

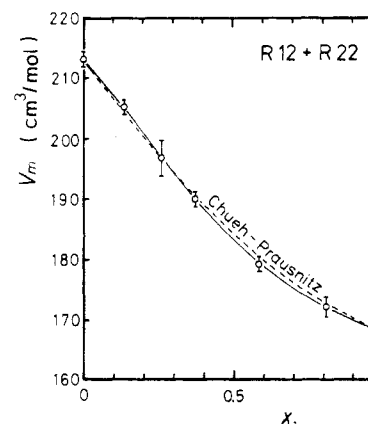


Figure 6. Composition dependence of the critical molar volume for the R12 + R22 system.

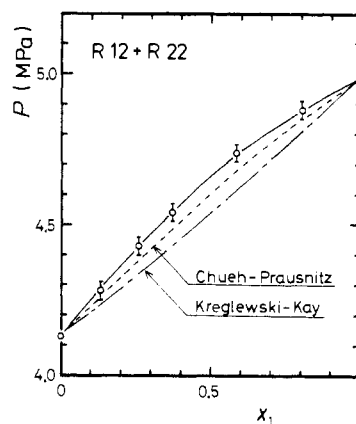


Figure 7. Composition dependence of the critical pressure for the R12 + R22 system.

$T-\rho$  plane for the mixtures between 75 and 100 wt % R22 would be depicted between two curves for 75 and 100 wt % R22 measured. It is noticeable that the critical locus between 75 and 100 wt % R22 both on the  $P-T$  plane and on the  $T-\rho$  plane bends much more sharply in comparison with the other portion of the locus. This feature of the critical locus might be explained in connection with the azeotrope which is formed in the present system in the temperature range below 258.65 K (7).

Figures 5–7 show the composition dependence of the critical temperature, molar volume, and pressure, respectively. In Figures 6 and 7 the estimated uncertainty of each value is also described as a gate. Mutual comparisons among different plots show that the critical loci on the  $T-x$  and  $V_m-x$  planes are

concave, whereas that on the  $P$ - $x$  plane is convex. Especially such behavior on the  $T$ - $x$  plane is remarkable. These critical loci are compared with the predictions recommended by Reid et al. (10), which are shown as broken and chain lines in Figures 5-7. With respect to  $T_c$ , two predictive methods by Li (11) and Chueh-Prausnitz (12) are compared with the present data. As shown in Figure 5, these predictions are much higher than the experimental data by about 0.5-1% and these cannot predict the concave behavior of the experimental data either. The critical molar volume  $V_{mc}$  predicted by the Chueh-Prausnitz method (12) is in good agreement with the present value within the estimated uncertainty. The prediction of  $P_c$  by the Chueh-Prausnitz method (12) is lower than the present  $P_c$  by about 0.5-1%, whereas that by the Kreglewski-Kay method (13) is much lower by about 1-2%.

The critical parameters of pure R12 have been reported by four different investigators. In 1931 Bichowsky and Gilkey (14) determined  $T_c = 384.65 \pm 0.5$  K by the direct observation of critical phenomena,  $\rho_c = 555$  kg/m<sup>3</sup> by extrapolating the rectilinear diameter to the critical temperature, and  $P_c = 4.008$  MPa by extrapolating their vapor pressure correlation. In 1955 McHarness et al. (15) determined  $T_c = 385.15$  K by observing the disappearance of the meniscus,  $\rho_c = 558.1$  kg/m<sup>3</sup> by the rectilinear diameter, and  $P_c = 4.115$  MPa by their vapor pressure correlation. Their sample purity used was not less than 99.95%. In 1966 Michels et al. (16) measured the compressibility isotherms for 99.95% R12 in the temperature range 273-423 K and for pressures up to 40 MPa. They determined  $T_c = 384.95 \pm 0.05$  K,  $\rho_c = 565 \pm 6$  kg/m<sup>3</sup>, and  $P_c = 4.125 \pm 0.005$  MPa by analyzing the isotherms measured in the critical region. In 1977 Rathjen and Straub (17) determined  $T_c = 384.93 \pm 0.015$  K for 99.98% R12 by visual observation of the reappearance of the meniscus. The present  $T_c$  value is higher than that of Rathjen and Straub and that of Michels et al. by 0.08 and 0.06 K, respectively, but is lower than that of McHarness et al. by 0.14 K. As for  $\rho_c$ , the present value differs from that of Michels et al. by only 0.5%.

The critical parameters of pure R22 have been reported by six different investigators. In 1935 Booth and Swinehart (18) measured the critical point when the meniscus disappeared in the center of the tube and determined  $T_c = 369.55 \pm 0.1$  K and  $P_c = 4.912 \pm 0.005$  MPa. In 1939 Benning and McHarness (19) determined  $T_c = 369.15$  K by the disappearance of the meniscus,  $\rho_c = 525$  kg/m<sup>3</sup> by the rectilinear diameter, and  $P_c = 4.935$  MPa by their vapor pressure correlation. They also reported that the temperature difference between the reappearance and disappearance of the meniscus was less than 0.4 K. In 1968 Zander (20) determined  $T_c = 369.33 \pm 0.02$  K for 99.97% R22 as the average temperature of the reappearance and disappearance of the meniscus. He adopted the critical density and pressure to be 513 kg/m<sup>3</sup> and 4.990 MPa, respectively. In 1971 Kletskii (21) determined  $T_c = 369.28 \pm 0.03$  K for 99.85% R22 as the maximum temperature at which a meniscus existed. He also determined  $\rho_c = 513 \pm 10$  kg/m<sup>3</sup> and  $P_c = 4.986 \pm 0.004$  MPa by the rectilinear diameter. In 1974 Hirata et al. (22) determined the critical parameters for 99.97% R22, being  $T_c = 369.30 \pm 0.05$  K by direct observation of the reappearance of the meniscus and  $P_c = 4.988 \pm 0.005$  MPa due to their vapor pressure correlation. In 1977 Rathjen and Straub (17) determined  $T_c = 369.27 \pm 0.015$  K for 99.98% R22 by visual observation of the reappearance of the meniscus. The  $T_c$  values measured recently including the present value agreed quite well within a difference of 60 mK and the present  $\rho_c$  value is also in good agreement with the values by Zander and Kletskii within 0.4%.

The critical exponent  $\beta$  along the coexistence curve can be determined on the basis of the power law representation

$$[(\rho^\pm - \rho_c)/\rho_c] = B[(T - T_c)/T_c]^\beta \quad (2)$$

where the plus sign indicates the saturated liquid and the minus sign the saturated vapor, and  $B$  denotes an adjustable parameter. Applying least-squares fitting to eq 2 for the range of reduced temperature difference  $1 \times 10^{-4} < |(T - T_c)/T_c| < 3 \times 10^{-2}$  for R12 and  $5 \times 10^{-5} < |(T - T_c)/T_c| < 3.5 \times 10^{-2}$  for R22, we obtained values of  $\beta$  and  $B$ , 0.337 and 1.872 for R12, and 0.348 and 1.996 for R22, respectively, based on the present data along the coexistence curve. Rathjen and Straub (17) measured the refractive index and determined the critical exponent  $\beta$  from the equation

$$(\rho^+ - \rho^-)/\rho_c = 2B[(T_c - T)/T_c]^\beta \quad (3)$$

They reported that the values of  $\beta$  and  $B$  were 0.3468 and 1.9364 for R12, and 0.3457 and 1.9545 for R22, respectively. No considerable difference of these values between Rathjen and Straub values and the present values is found.

#### Acknowledgment

We are greatly indebted to Mitsui Fluorochemicals, Co., Ltd., Tokyo, Japan, for kindly furnishing the sample and also to the National Research Laboratory of Metrology, Ibaraki, Japan, for the calibration of the thermometer. The assistance of Ken-ichi Fujii, who made the elaborate observations with the present authors, is gratefully acknowledged.

#### Glossary

$B$	adjustable parameter in eq 2 and 3
$m$	mass, kg
$P$	pressure, MPa
$P_c$	critical pressure, MPa
$T$	temperature, K
$T_c$	critical temperature, K
$T_r$	reduced temperature = $T/T_c$
$V$	inner volume of a vessel, cm <sup>3</sup>
$V_m$	molar volume, cm <sup>3</sup> /mol
$V_{mc}$	critical molar volume, cm <sup>3</sup> /mol
$x$	mole fraction
$x_1$	mole fraction of R22
$w_1$	mass fraction of R22
$\beta$	critical exponent along the coexistence curve
$\rho$	density, kg/m <sup>3</sup>
$\rho_c$	critical density, kg/m <sup>3</sup>
$\rho_r$	reduced density = $\rho/\rho_c$
$\rho^+$	saturated-liquid density, kg/m <sup>3</sup>
$\rho^-$	saturated-vapor density, kg/m <sup>3</sup>

Registry No. CCl<sub>2</sub>F<sub>2</sub>, 75-71-8; CHClF<sub>2</sub>, 75-45-6.

#### Literature Cited

- (1) Kriebel, M. *Kaeltetechn.-Klim.* **1967**, *19*, 8.
- (2) Takaishi, Y.; Kagawa, N.; Uematsu, M.; Watanabe, K. *Proc. Symp. Thermophys. Prop.*, 8th **1962**, *2*, 387.
- (3) Takaishi, Y.; Uematsu, M.; Watanabe, K. *Bull. JSME* **1962**, *25*, 944.
- (4) Takaishi, Y.; Kagawa, N.; Uematsu, M.; Watanabe, K. *Nippon Kikai Gakkai Ronbunshu, B Hen* **1963**, *49*, 2803.
- (5) Kagawa, N.; Takaishi, Y.; Uematsu, M.; Watanabe, K. *Nippon Kikai Gakkai Ronbunshu, B Hen* **1963**, *49*, 2811.
- (6) Okazaki, S.; Higashi, Y.; Takaishi, Y.; Uematsu, M.; Watanabe, K. *Rev. Sci. Instrum.* **1963**, *54*, 21.
- (7) "Thermophysical Properties of Refrigerants (R12, Dichlorodifluoromethane)", Japanese Association of Refrigeration, Tokyo, 1981.
- (8) "Thermophysical Properties of Refrigerants (R22, Chlorodifluoromethane)", Japanese Association of Refrigeration, Tokyo, 1975.
- (9) Takaishi, Y. Ph.D. Thesis, Keio University, Yokohama, Japan, 1982.
- (10) Reid, R. C.; Prausnitz, J. M.; Sherwood, T. K. "The Properties of Gases and Liquids", 3rd ed.; McGraw-Hill, New York, 1977.
- (11) Li, C. C. *Can. J. Chem. Eng.* **1971**, *49*, 709.
- (12) Chueh, P. L.; Prausnitz, J. M. *AIChE J.* **1967**, *13*, 1099.
- (13) Kreglewski, A.; Kay, W. B. *J. Phys. Chem.* **1969**, *73*, 3359.
- (14) Bichowsky, F. R.; Gilkey, W. K. *Ind. Eng. Chem.* **1931**, *23*, 366.
- (15) McHarness, R. C.; Eiseman, B. J., Jr.; Martin, J. J. *Refrig. Eng.* **1955**, *63*, 31.

- (16) Michels, A.; Wassenaar, T.; Wolkers, G. J.; Prins, Chr.; Klundert, L. v. d. *J. Chem. Eng. Data* **1966**, *11*, 449.  
 (17) Rathjen, W.; Straub, J. *Proc. Symp. Thermophys. Prop.*, 7th **1977**, 839.  
 (18) Booth, H. S.; Swinehart, C. F. *J. Am. Chem. Soc.* **1935**, *57*, 1337.  
 (19) Benning, A. F.; McHarness, R. C. *Ind. Eng. Chem.* **1939**, *31*, 912.  
 (20) Zander, M. *Proc. Symp. Thermophys. Prop.*, 4th **1968**, 114.

- (21) Kletskii, A. V. "Thermophysical Properties of Freon-22"; Israel Program for Scientific Translations: Jerusalem, 1971.  
 (22) Hirata, M.; Nagahama, K.; Saito, J.; Wakamatsu, N. *Prepr. 8th Autumn Meeting Soc. Chem. Eng., Jpn.* **1974**, 444.

Received for review January 3, 1983. Accepted July 18, 1983.

## Solubility of Carbon Monoxide in 1,4-Dioxane

Ewald Veleckis\* and David S. Hacker†

Argonne National Laboratory, Argonne, Illinois 60439

The solubility of CO in 1,4-dioxane was determined as a function of pressure (7–70 atm) and temperature (80–173 °C). Solubility data can be represented by the equation  $x_2 = (2.025 \times 10^{-3} - 0.4974T^{-1})P_2 + [-2.574 \times 10^{-6} + (7.351 \times 10^{-4})T^{-1}]P_2^2$ , where  $x_2$  and  $P_2$  are the mole fraction and the partial pressure of CO (in atmospheres), respectively, and  $T$  is the Kelvin temperature. The results, analyzed in terms of the Krichevsky–Ilinskaya equation, showed that the partial molar volume of CO was independent of pressure and that the isobaric Henry's law was obeyed in the ranges studied. The temperature dependence of the Henry's law constant may be expressed by  $\ln H_{2,1} = 5.688 + 594.6T^{-1}$  where  $H_{2,1}$  is atm (mole fraction of CO)<sup>-1</sup>. Comparisons with other solvents showed that, on the basis of CO dissolution characteristics, 1,4-dioxane can be classified better with polar than with nonpolar solvents.

### Introduction

The solubility of hydrogen and carbon monoxide in organic solvents is of interest in certain applications of the Fischer–Tropsch (FT) catalytic synthesis of hydrocarbons, where an optimum solvent must be selected to serve as a suspending medium for the slurried catalyst (1). Reliable solubility data on these two gases at the conditions of the synthesis (~1000 psi, ~250 °C) are sparse. For example, in the case of CO, a recent compilation (2) cites solubility data for only 16 solvents, most data being taken at moderate temperatures and pressures. The present study was undertaken to investigate  $P$ – $C$ – $T$  relationships for solutions of CO in 1,4-dioxane, one of the solvents used in the slurried FT catalysis. A survey of the literature revealed no previous work on this system.

### Experimental Section

**Chemicals.** Carbon monoxide (99.99+ %) was supplied by the Matheson Co., Inc., and was used without any further compression and purification; 1,4-dioxane (spectrophotometric grade, 99+ %) was purchased from the Aldrich Chemical Co. Prior to introduction into the autoclave, the liquid was degassed according to a procedure suggested by Battino et al. (3): the vigorously agitated liquid was subjected to a series of brief exposures to vacuum until all air was extracted as indicated on a vacuum gauge connected to the liquid container via a cryogenic trap.

**Apparatus and Procedure.** The solubility of CO in 1,4-dioxane was measured in a 2-L stainless-steel autoclave (Autoclave Engineers, Erie, PA, Model AFP-2005) equipped with (1)

a magnetically driven stirrer; (2) a pressure transducer (Validyne Engineering Corp., Northridge, CA, Model P-10, 1250 psi range), calibrated against a dead-weight standard; (3) a chromel–alumel thermocouple, calibrated against a platinum resistance thermometer; (4) inlets for the gas and liquid; and (5) a 0.062-in.-i.d. liquid-sampling tube that extended to a point located near the bottom of the autoclave. The autoclave was heated with a jacket-type furnace. Temperature of the liquid sample in the autoclave could be controlled to within  $\pm 0.5$  °C.

Approximately 1 L of degassed 1,4-dioxane was introduced into the previously evacuated autoclave, which was then pressurized with CO and heated to the desired temperature. The mixture was equilibrated while a steady stirring rate of 250 rpm was maintained. The attainment of the equilibrium was judged to be complete when the pressure remained constant for a period of at least 1 h. The time to reach equilibrium ranged from 1 h at 173 °C to 10 h at 80 °C.

The saturated liquid was sampled by withdrawing a small quantity from the autoclave, via a metering valve, at the rate of  $\sim 8$  mL min<sup>-1</sup>. The initial portion of the sample ( $\sim 6$  mL) was always discarded by directing the liquid flow into a special container. The sample itself (8–12 mL) was collected in a previously evacuated buret system. Upon entering the burets, the gas flashed out of solution and produced two distinguishable phases, which were then compressed to atmospheric pressure, mercury being used as the leveling fluid. All gas–liquid–mercury interfaces were recorded with the aid of a cathetometer. The quantities of the separated gas and liquid phases were calculated from their respective volumes, buret-system temperature, barometric pressure, and density of 1,4-dioxane ( $d_{20^\circ\text{C}} = 1.0337$  g cm<sup>-3</sup> (4)). After the measurements, gas pressure in the autoclave was changed to a new value and the buret system was cleared in preparation for the next sampling.

The buret system used in the sample analysis was similar to one described by Wiebe et al. (5, 6). It comprised two calibrated, connected burets (50- and 100-mL capacity) enclosed in a thermostated water jacket. Gas volumes in the burets could be individually varied by controlling the mercury levels. Volume measurements were precise to within  $\pm 0.2$  mL.

Stirring of the liquid during sampling was necessary to maintain a uniform temperature distribution. Samples taken at different stirring rates (250–500 rpm) showed no variation in the quantity of the dissolved CO. Slight reduction in the autoclave pressure caused by the sample removal was assumed to have no effect on the CO concentration because the response time of the solution toward changes in pressure was comparatively slow. For example, at 96 °C and 70-atm pressure, >2 h would have been required to compensate for a 1.5-atm pressure deficit encountered during a typical sampling operation.

The transducer used for measuring autoclave pressures was located outside the heated zone and was connected to the autoclave via a 30-in.-long, 0.062-in.-i.d. tube. Some question

\* Present address: Amoco Chemicals Corp., Naperville, IL 60566.